



Characterization of cork and cork agglomerates under compressive loads by means of energy absorption diagrams

Ramon Miralbes¹ · David Ranz¹ · Jan Ivens² · Jose Antonio Gomez¹

Received: 6 April 2020 / Accepted: 2 November 2020 / Published online: 17 November 2020
© Springer-Verlag GmbH Germany, part of Springer Nature 2020, corrected Publication 2020

Abstract

Cork and cork agglomerates could be suitable replacements for petroleum-based polymeric foams due to their similar internal structure of cells and grains. Additionally, cork products have a renewable origin and are recyclable. Despite these notable properties, few studies have analysed the mechanical properties, especially the specific properties, of these materials under compressive loads. Moreover, although efficiency, ideality, and energy-normalized stress diagrams are commonly used for polymeric foams and 3D-printed lattice structures, these types of diagrams are not yet applied to cork products. It must be highlighted that efficiency diagrams are plotted only against nonspecific properties so, this article proposes additionally the use of nonspecific properties to compare materials not only in terms of properties per unit volume instead but also in terms of properties per unit mass that is more suitable for certain applications in which the weight is crucial. The materials studied herein include three different white cork agglomerates, a brown cork agglomerate, a black cork agglomerate, natural cork, and expanded polystyrene foam, which are subjected to quasi-static compressive loads.

1 Introduction

Cork and cork agglomerates have been reported by many authors (Chua et al. 2017; Coelho et al. 2012) as a possible substitute for polymeric foams in certain applications where the material needs to absorb energy to protect other elements, such as in helmet liners (de Sousa et al. 2012) and packaging applications. The main advantage of cork and cork agglomerates is that they are of renewable origin and they can be easily recycled to produce new cork agglomerates (Knopic et al. 2016). Moreover, in contrast to polymeric foams, especially expanded polystyrene (EPS) which has low resilience, cork and cork agglomerates recover their initial shape after high strains (Maderuelo-Sanz et al. 2014). Consequently, cork and cork agglomerates are adequate materials for the use as protection material in applications that might need to absorb multiple impacts (Fernandes et al. 2019).

One of the main disadvantages of natural cork is that, due to its natural origin, there is substantial variability in its material properties (González-Hernandez et al. 2014; Lauw et al. 2018) and density (Silva et al. 2005). The former disadvantage can be overcome in cork agglomerates because the material properties can be tailored (Santos et al. 2017) by selecting the binder type, the grain size, and the volume fraction of the cork and the binder.

In terms of mechanical properties, many authors have studied the influence of several factors such as the porosity, density, and quality (Anjos et al. 2011) on the mechanical properties of cork products; these factors depend ultimately on the cork oak. In the same way, other authors (Crouvisier-Urion et al. 2018) have studied the influence of some agglomerate design parameters mentioned in the previous paragraph.

These studies also revealed that, when subjected to compressive loads, cork and cork agglomerates exhibit a characteristic stress–strain curve that is similar to that of polymeric foams and that was defined as the Gibson’s model (Gibson and Ashby 1997) for these latter materials. However, the transition points between the elastic and plateau zones of cork and cork agglomerates are not as well defined (Fernandes et al. 2015), and these cork materials usually exhibit reduced slopes in the elastic zone and higher slopes in the plateau zone.

✉ Ramon Miralbes
miralbes@unizar.es

¹ Department of Design and Manufacturing, University of Zaragoza, Zaragoza, Spain

² Department of Design and Manufacturing, KU Leuven, Leuven, Belgium

For polymeric foams, which are created by a foaming process, the relationship between the density and the mechanical properties is well known (Doroudiani and Kortschot 2003; Chen et al. 2015). Hence, it is possible to tailor the mechanical properties of polymeric foams because the desired final density can be obtained by controlling the expansion process and the amount of air trapped inside the foam.

Foams, cork, and cork agglomerates, as previously noted, can be defined using the Gibson model (Gibson and Ashby 1997) (see Fig. 1), which establishes three well-defined parts of the stress–strain curve under compressive loads: the elastic zone, the plateau zone, and the densification zone. In the elastic zone, the material can recover its initial shape and its behaviour is defined by Young’s modulus. In the plateau zone, the cells in the material progressively collapse. In this stage, polymeric foams usually exhibit constant stress or a curve with a very low increasing slope, whereas cork and cork agglomerates usually exhibit a constantly increasing curve (Anjos et al. 2014) with a slope that is significantly higher than that of the curve for polymeric foams (Fernandes et al. 2015). Hence, this zone is significantly better suited for energy absorption than the elastic zone (Wilhelm et al. 2017). In the plateau zone, polymeric foams, which usually have closed cells, cannot recover their initial shape. In contrast, cork and cork agglomerates, which have open cells, can recover most of their initial shape.

The densification zone appears when all the air trapped inside is expelled and so, the opposing walls in the cells collide; consequently, the stress increases steeply (see Fig. 1).

The main parameters of the stress–strain curves are as follows:

- Maximum tensile strength in the elastic zone ($\sigma_{c,e}$)
- Maximum tensile strength at the densification point ($\sigma_{c,d}$)
- Maximum elastic elongation ($\epsilon_{c,p}$)

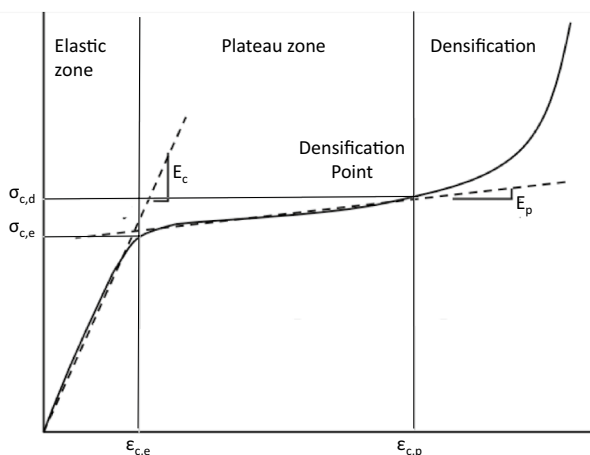


Fig. 1 Typical stress–strain curve for EPS

- Elongation at the densification point ($\epsilon_{c,d}$)
- Elastic Young’s modulus (E_c)
- Plateau Young’s modulus (E_p)

The total energy absorbed per unit of volume by the material can be obtained from below equation:

$$W = \int_0^{\epsilon_i} \sigma d\epsilon \quad (1)$$

This total energy absorption can be decomposed in the following two components:

$$\text{Elastic energy absorption } W_e = \int_0^{\epsilon_{c,p}} \sigma d\epsilon \quad (2)$$

$$\text{Energy absorbed in the plateau zone } W_p = \int_{\epsilon_{c,p}}^{\epsilon_{c,d}} \sigma d\epsilon \quad (3)$$

Traditionally, there are some considerations that are involved in the design of an effective energy absorber, such as the geometry and the material of the protection device. However, currently, products must also be environmentally friendly; hence, petroleum-based polymeric foams should be replaced, and cork and cork agglomerates are promising for this purpose (Tay et al. 2014). One of the main drawbacks of this type of material is that, although many different studies have been performed on cork and cork agglomerates under compressive loads, these studies mainly focused on one or a few similar types of cork or cork agglomerates. For example, Fernandes et al. (2019) compared two white agglomerates with different grain sizes and an expanded black agglomerate with different EPS foams. Lagorde-Tachon et al. (2017) studied the effect of hydration of natural cork. Anjos et al. (2014) analysed the influence of the density of natural cork. Jardin et al. (2015) investigated the behaviour of four white cork agglomerates and three black cork agglomerates.

The main problem in these studies is that they do not consider weight in mechanical analysing. Hence, these studies did not investigate the specific mechanical properties, which is essential for certain applications. For instance, in helmets, weight reduction can help reduce the rotational accelerations and rotational moments that significantly contribute to head injuries (Hajiaghmemar et al. 2020). Additionally, previous studies did not examine some parameters, such as the efficiency, ideality, normalized stress and normalized absorbed energy.

It must also be highlighted that these studies did not compare natural cork and white agglomerates, brown agglomerates, and black agglomerates with different grain sizes.

Recently, other authors have applied multi-scale analysis based on the study of the microstructure to determine mechanical behaviour. The microstructure has been determined using scanning-electron and optical microscopy and X-ray tomography (Le Barbenchon et al. 2019) on two different scales: cells and beads to determine some variables of the agglomerates (particle shape and size, particle orientation, particle arrangement, etc.). Then, using this information, it is possible to create a parametric numerical model using the finite element method of a representative volume element to reproduce the mesostructure of the agglomerate (Delucia et al. 2020a, b). This numerical model includes the mechanical properties of the natural cork and the binder to obtain some of the mechanical properties of the resultant agglomerate such as Young's modulus, shear modulus, Poisson's ratio, and thermal conductivity depending on the volume fraction; additionally, it is possible to also obtain the elastic properties depending on the temperature (Delucia et al. 2020b). Consequently, this method allows to predict some of the mechanical properties of cork agglomerates without any experimental test using only non-intrusive methods and the properties of the constitutive materials. In the same way, it will be possible to tailor the agglomerate to obtain the desired mechanical properties using the parameters obtained from the numerical simulation. Whilst these techniques are promising, one of the main drawbacks nowadays is that they can just only predict Young's modulus but not all the stress–strain curve.

Another aspect to mention is related to the effect of the strain rate on the mechanical properties. The research of Ptak et al. (2017) illustrates the influence of the impact velocity and, consequently the strain rate on the stress–strain curve. Whilst an increase in the strain rate implies higher stress levels and a higher capability to absorb energy, the elongation in the densification point is lower so the densification appears earlier. In the same way, a higher strain rate implies higher contact forces (Sanchez-Saez et al. 2015). Whilst this aspect should be studied, this article is focused only on the quasi-static test. In the same way, although the temperature also modifies the mechanical properties of these materials (Ptak et al. 2018), the article only studies the materials at room temperature (20 °C).

To sum up, the objective of this paper is the comparative analysis of different cork agglomerates, natural cork and an EPS foam under compression quasi-static loads to determine the capability to absorb energy per unit of weight and per unit of volume to quest whether these materials can substitute the EPS. Additionally, the use of some variables such as the effectivity and the ideality were explored to select the most suitable material; these variables weigh the required energy absorption, the maximum allowed stress and the strain. Additionally, the influence of the strain at the densification point

on the efficiency was explored and whether this variable could be used to determine the densification point.

Moreover, it was explored whether these materials follow Gibson's model and the influence of the density on the strain at the densification point. The main hypothesis is that heavier agglomerates have less air trapped inside and, consequently, the densification appears earlier and it has a higher stiffness. Another hypothesis is that natural cork, due to the fact that its natural internal structure is intact, has higher specific and nonspecific mechanical properties than the cork agglomerates but, due to the lower quantity of air trapped inside, the densification appears earlier.

2 Materials and methods

2.1 Materials

The materials studied are natural cork (NC), three different white cork agglomerates (WCAs), a black agglomerate (BCA) and a brown cork agglomerate (BCA) (Table 1 and Fig. 2), which have different densities and grain sizes (see Fig. 1). For comparison, this table also lists the properties of a 75 kg/m³ expanded polystyrene foam (EPS75), which is commonly used for the helmet liners. The common density of EPS in helmet liners varies between 60 and 120 kg/m³.

Natural cork sheets are the external bark of the oak tree, which is removed using cutting machines and axes to produce flat regular sheets. The variation in the dimensions of these sheets primarily depends on the tree itself and—to a lesser extent—on the cutting process. Commercially, the common sheet thickness ranges between 3 and 15 mm and the sheet width and length range between 100 and 600 mm. One of the main drawbacks of natural cork, due to its natural origin, is that its mechanical properties can vary substantially (Oliveira et al. 2014).

Natural cork and/or recycled cork can be mechanically chopped into granules and sifted and then joined under pressure and heated to obtain cork agglomerates which have more stable mechanical properties. These materials are formed into regular sheets and bricks with fewer shape and dimension limitations than the base materials. These materials have different mechanical properties depending on the size of the granules and the binder used. There are different types of cork agglomerates: white, black and brown.

Although white cork agglomerates can be obtained using biodegradable water-based glues, these agglomerates are most commonly obtained using no biodegradable resins, such as phenolic and vinyl resins, polyester, and epoxy. Consequently, these materials are no longer completely renewable.

Brown cork agglomerates are manufactured using the same process as white cork agglomerates, but they use

Table 1 Studied materials, their grain size and density and mechanical properties of constitutive materials

Designation		Reported density (kg/m ³)	Actual density (kg/m ³)	Grain size (mm)	Resin volume fraction (%)	Binder
EPS75	Exp. polystyrene	70	71.1	2–3		None
WCA300	White agglomerate	300	302	0.5–2	5	Polyurethane
WCA275	White agglomerate	275	279	1–3	7	Polyurethane
WCA230	White agglomerate	230	222	2–5	10	Polyurethane
BCAC170	Brown agglomerate	170	172	2–5		Suberin
BCA100	Black agglomerate	100	104	4–10		Suberin
NC260	Natural cork	260	263	None		None
Material (binder/origin)		Young's modulus (MPa)	Poisson's ratio	Density (kg/m ³)	Tensile strength (MPa)	Maximum elongation (%)
Polyurethane		8.6	0.48	1320	28	368
Polystyrene		3250	0.325	1080	37	1.6
Natural Cork		29.6	0.0	263	3.5	12

References of materials used:

EPS75: Lazersports. <https://www.lazersport.com/en>

WCA300: <https://www.barnacork.com/placas-de-corcho/placas-de-corcho/placas-de-corcho-grano-fino.html>

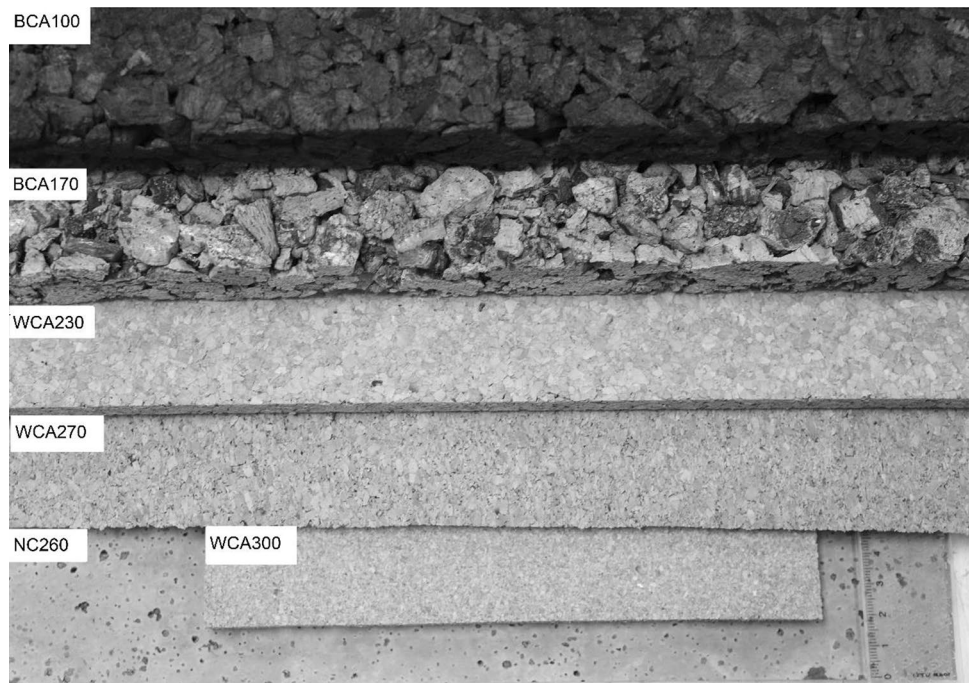
WCA275: <https://www.barnacork.com/placas-de-corcho/placas-de-corcho/placas-de-corcho-610-x-450-mm.html>

WCA230: <https://www.barnacork.com/placas-de-corcho/placas-de-corcho/placas-de-corcho-grano-grueso.html>

BCA 170: <https://www.barnacork.com/aislamientos/aislamientos/aglocork-acustico-natural.html>

BCA100: <https://www.barnacork.com/aislamientos/aislamientos/aglocork-fachadas.html>

NC 260: <https://www.barnacork.com/corcho-natural/corcho-natural/laminas-de-corcho-natural.html>

Fig. 2 Studied cork and cork agglomerates

suberin, a resin naturally exuded from cork, as a binder. It must be noted that this binder has low mechanical properties that negatively affect the behaviour of the whole material, especially under traction loads (Paiva and Magalhaes 2018).

Black cork agglomerates are manufactured by means of pressure combined with high-temperature steam. As a result, the grains expand (which is why this material is also called “expanded cork”), and the suberin extracted from the granules acts as a binder.

The studied natural cork is commercialized in 600 mm × 100 mm × 10 mm sheets. The three white cork agglomerates with different binders and densities are presented in 915 mm × 610 mm × 10 mm sheets. Both the black cork agglomerate and the brown cork agglomerate are commercialized in 1000 mm × 500 mm × 20 mm sheets.

2.2 Methods

There is not a specific standard to test cork agglomerates. However, ASTM D3574 “Standard Test Methods for Flexible Cellular Materials-Slab, Bonded, and Molded Urethane Foams”, ASTM D1621 “Standard Test Method for Compressive Properties of Rigid Cellular Plastics” and ISO 844 “Rigid Cellular Plastics Compression Properties” could be applicable to these materials. EPS75, which is a rigid cellular plastic, has similarities to the cork materials; hence the above-mentioned standards could also be applicable to cork products.

All the aspects of the standards, including the prismatic shape of the specimens, are similar except for the minimum and/or preferred specimen dimensions. In ASTM D1621, the minimum specimen is a 25.4 mm cube, while in ASTM D3574, the preferred specimen is a 50 mm × 50 mm × 25 mm prism and in ISO 844, the preferred one is a 100 mm × 100 mm × 50 mm prism, for which

the minimum allowed thickness is 50 mm. Due to the fact that there are certain sheet thickness limitations that were previously mentioned in the Materials section, ASTM D1621 was used; as a result, finally, a prismatic shape with a 50 mm × 50 mm cross-section and the maximum thickness was adopted. All the specimens were machined using a Roland MDX 20 CNC milling machine and a minimum finishing allowance of 10 mm was used.

It must also be mentioned that the adopted test methodology and the specimen dimensions are similar to those used by the authors of the abovementioned cork and EPS compression studies.

Consequently, the materials are tested under quasi-static compression with a 5 mm/min crosshead displacement rate using an 8032 INSTRON universal machine which has coupled 150 mm compression platens to test the specimens; this displacement rate was obtained from the mentioned standards; all of them specify the same displacement rate and, as a result, the specimens are tested with a strain rate of 0.0083/s. This INSTRON machine records the forces and displacements during testing, which are used to determine the stress–strain curve and the other diagrams using the geometric dimensions of the specimens.

Three specimens of each material were tested to analyse the variability of the results and it was observed that the variability of the results is less than 5% for all the materials. The stress–strain curve has been obtained using the average value of the curves of the three specimens.

2.3 Interpretation of the results

Some authors, such as Avalor et al. (2001), proposed the use of different energy-absorption diagrams to select, compare, and tailor polymeric foams using the density to obtain the optimal mechanical properties. These diagrams (see Fig. 3)

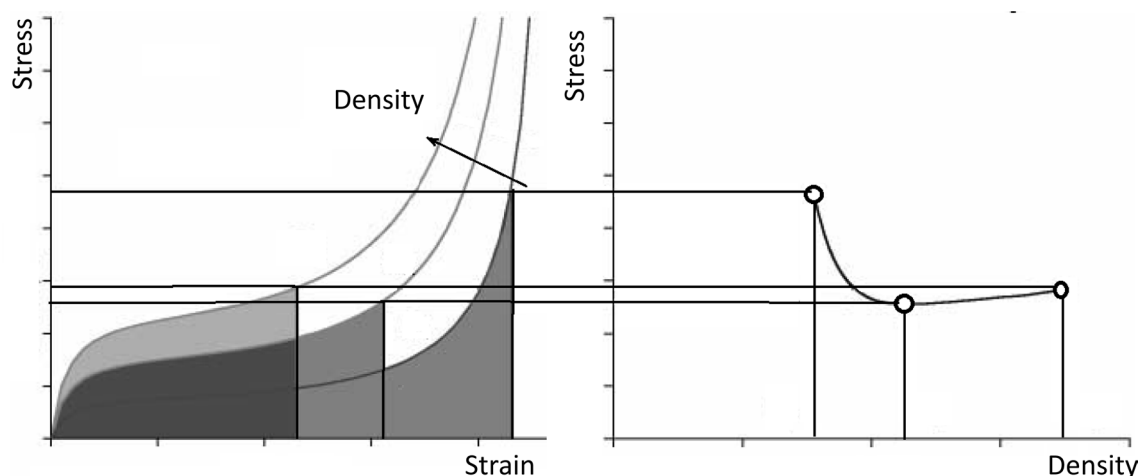


Fig. 3 Typical (left) stress–strain diagrams and (right) maximum stress–density for a polymeric foam

are based on the stress–strain curve, which could be used to obtain the energy and the maximum stress. Additionally, they can be used to verify whether the densification point is reached.

Note that the absorbed energy is the area below the stress–strain curve and can be defined using Eq. 1.

Figure 3 shows that polymeric foams typically exhibit a behaviour that is characterized by an increase in the stress values ($\sigma_{c,e}$, $\sigma_{c,d}$) in the different zones of the curve and the capability to absorb energy (W_p) when the density increases. However, the increase in the density of the foam (which is directly related to the reduction in the amount of air trapped inside the foam) suggests that the densification point is reached earlier (reduction in $\varepsilon_{c,d}$) and, after this point, the stress increases exponentially.

Additionally, Fig. 3 shows that to absorb the same amount of energy (W_{abs}), if the material is too stiff (high density), then higher stress appears because the curve in the plateau zone is higher and the final strain is far from the

densification point. Hence, the material has not been properly used because it has the capability to absorb more energy without increasing the stress or it is possible to use a lower density foam that can absorb the same quantity of energy with lower stress levels. Conversely, if the material is not sufficiently stiff (density is too low), the material deforms excessively and the densification point is passed so the stress increases exponentially and, in the end, higher stress levels are reached. An optimum point would be between these densities and then, the material would use all the capability of the plateau zone to absorb energy. This material would accomplish $W_{abs} = W_e + W_p \approx W_p$ because, compared with W_p , W_e could be negligible. It must be noted that the energy discussed is the amount of energy per unit volume.

Using the absorbed energy, it is possible to obtain the energy absorption–stress curve (Fig. 4), which can be used to verify the maximum stress that can be reached by the material to absorb a certain amount of energy. Due to the shapes of the stress–strain curves for polymeric materials

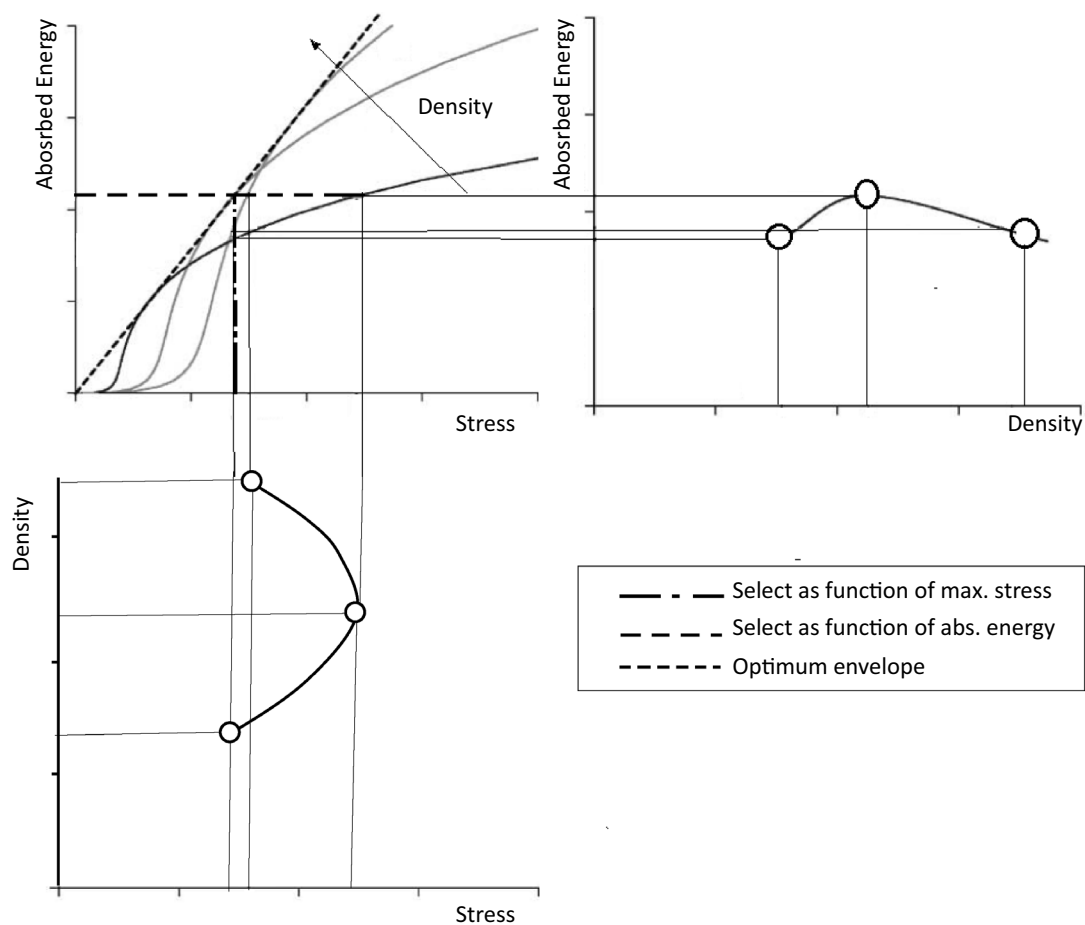


Fig. 4 Typical absorbed energy–stress (top-left), absorbed energy–density for a certain stress (top-right) and density–stress for a certain energy (bottom-left) diagrams for a polymeric foam

of the same type but different densities, it can be observed that it is possible to obtain an optimal envelope curve, which indicates the optimal point for each material; this optimal envelope is useful to determine the material (density of the foam) which can absorb the maximum amount of energy with the lowest stress. Avalle et al. (2001) mathematically demonstrated that the optimal envelope curve for this type of material is a constantly increasing line that begins at the origin. Accordingly, the optimal point (σ_{opt}) for this material will be close to $\sigma_{c,d}$.

These diagrams can also be used to select a material depending on the amount of energy that has to be absorbed and sustains the lowest stress (horizontal line) and also to obtain the material that can absorb more energy without passing a maximum defined stress (vertical line). It can be observed that the foam with the highest or lowest energy absorption in certain cases is not the optimum one.

Another interesting indicator proposed by Miltz and Ramon (1990) is efficiency (E), which is the ratio of the absorbed energy divided by the stress and is defined by this equation:

$$E = \frac{\int_0^{\epsilon_i} \sigma d\epsilon}{\sigma_i} \tag{4}$$

This parameter is usually plotted against strain (Fig. 3). Avalle et al. (2001) mathematically demonstrated that, for

the same type of foam with different densities, the optimal efficiency is constant (Fig. 5). This diagram can be used to select the most efficient material for certain maximum stress and using the iso-energy curves, it is possible to select the most efficient material or the material that has lower stress. It can be observed that, for a certain stress (vertical line) or for a certain amount of energy absorption, the most efficient material is in some cases not the lighter or the heavier one. In the same way, for a certain energy, the most efficient material implies the lowest stress levels.

Hansen et al. (1999, 2000) demonstrated that, although efficiency is useful for most common polymeric foams, there are some cases when the stress–strain curve does not monotonically increase, so, the efficiency does not take into consideration the previously reached stress, and, as a result, the efficiency is not an adequate indicator. For these cases, the total efficiency (E_t), which is the ratio of the energy W to the maximum experienced stress, was proposed to solve this drawback. The associated diagrams will be similar to efficient ones.

$$E_t = \frac{\int_0^{\epsilon_i} \sigma d\epsilon}{\max_{0 \leq \nu \leq \epsilon_i} \sigma_i} \tag{5}$$

This indicator is useful for certain types of lattice structures generated by additive manufacturing (Maskery et al.

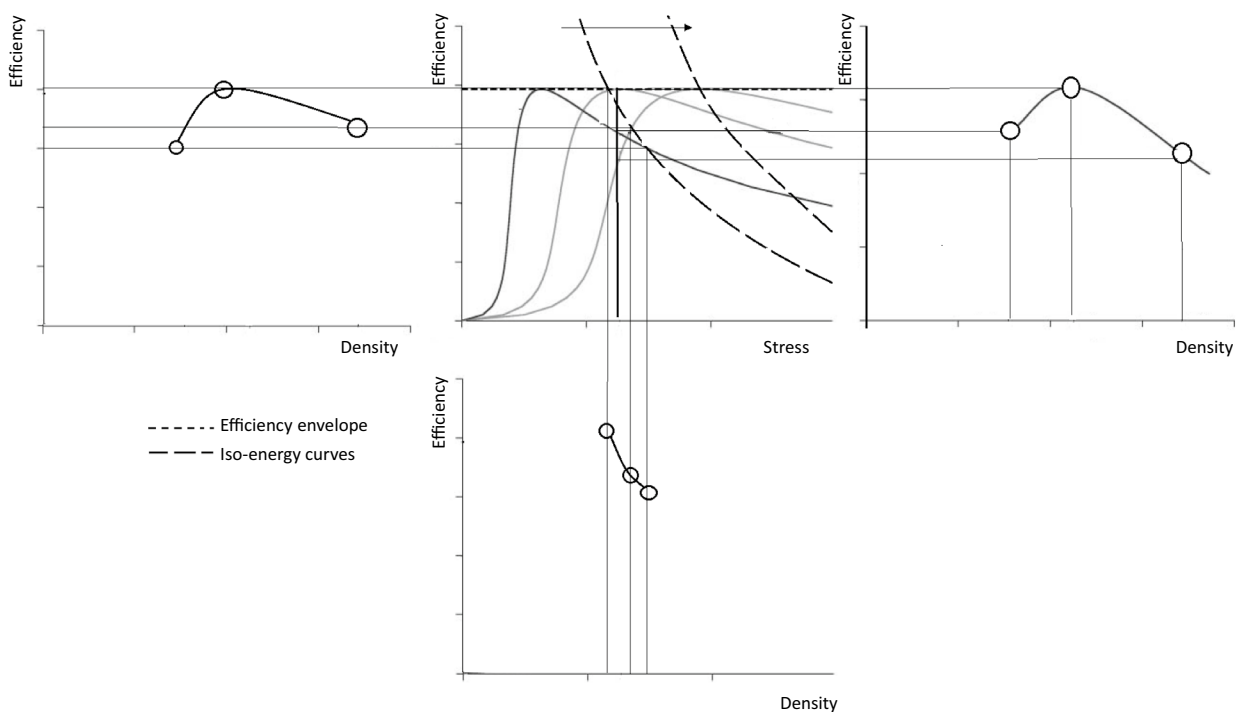


Fig. 5 Efficiency-stress curve and efficiency-density related curves

2017). In this particular case, the curves are monotonically increasing, so both indicators are identical.

Another indicator proposed by Miltz and Ramon (1990) was the ideality (I), which is defined in Eq. 6:

$$I = \frac{\int_0^{\varepsilon_i} \sigma d\varepsilon}{(\sigma_i \times \varepsilon_i)} \quad (6)$$

Ideality is another ratio of the efficiency that takes into consideration both the stress and the strain and analyses how close the material is to an ideal absorber (which has constant stress for all strains). However Miltz and Ramon (1990), discovered that the maximum value of this indicator for polymeric foams appears with low strain, usually at the beginning of the plateau. Consequently, these materials do not use all their energy-absorbing capability across the plateau zone and exhibit very low deformation. Hence, this indicator is not adequate for selecting these types of materials.

Other interesting parameters, such as the Janson factor (Gibson and Ashby 1997) or the cushion factor (Gibson and Ashby 1997), were proposed based on the Rush model (Rush 1969, 1970a, b), but they are not extensively used due to the difficulties in adjusting the Rush material model.

It must be highlighted that all of the abovementioned diagrams are useful to select materials for a specific volume. Nevertheless, in some applications, such as helmet liners, it is equally or more important to select a material to obtain a product with the lowest weight. Then, instead of using the stress and the energy, the specific stress (σ_s) and the specific energy (W_s) are more adequate. It is easy to demonstrate mathematically that ideality and efficiency do not change if the specific stress and the specific energy are used. It is also possible to obtain density (ρ)-specific properties, i.e., dividing the material parameters by the density.

To sum up, nonspecific parameters are used to compare different materials with the same volume and specific parameters are used to compare materials with the same weight.

The specific parameters are:

- Maximum specific compression strength in the elastic zone ($\sigma_{cs,e}$)
- Maximum specific compression strength at the densification point ($\sigma_{cs,d}$)
- Specific elastic Young's modulus (E_{cs})
- Specific plateau Young's modulus (E_{ps})
- Specific elastic absorbed energy (W_{es})
- Specific energy absorbed in the plateau zone (W_{ps})

Finally, there are some authors (Yu et al. 2019; Maskery et al. 2017) who used the normalized energy (W/E_{cb}) versus the normalized stress (σ/E_{cb}) and presented them in a double logarithmic diagram. These diagrams are useful to compare different materials that are generated using a foaming process or to compare different 3D printed hollow structures (such as the lattice ones) but with the same origin material. It must be pointed out that E_{cb} is Young's modulus of the non-foamed material in the case of the foams and, in the case of 3D printed materials, the Young's modulus of a solid specimen.

In the particular case of cork agglomerates, the original material would be natural cork and, consequently, E_{cb} is obtained from the stress–strain curve of NC260.

3 Results and discussion

All the results plotted in the following figures (Figs. 6, 7, 8 and 9) refer to the materials listed in Table 1.

The analysis of the stress–strain diagram (left side of Fig. 6) shows that the cork and the cork agglomerates exhibit a constantly increasing tendency, instead of a flat plateau as in the EPS. Moreover, the cork and cork agglomerates have a lower slope than the EPS in the elastic zone. Additionally, densification appears earlier in the cork

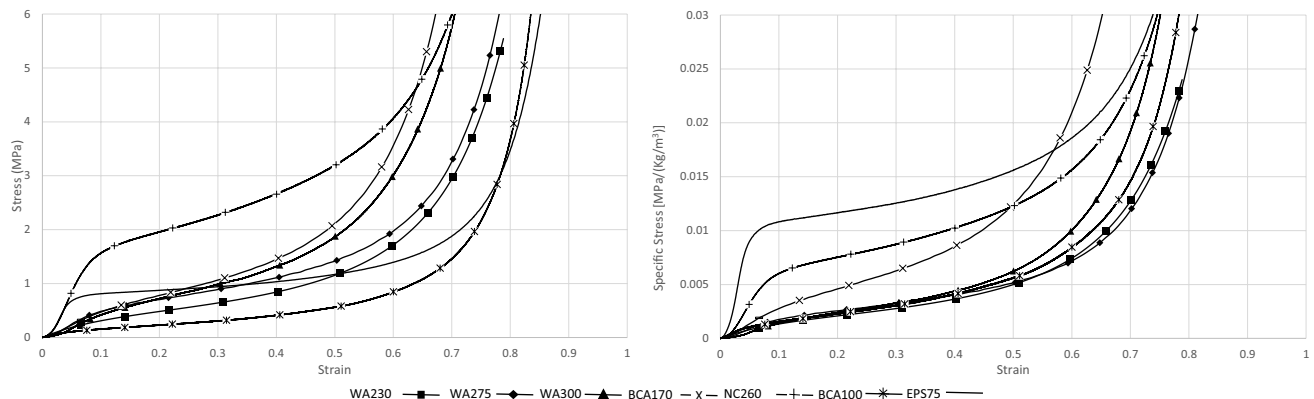


Fig. 6 (left) Stress–strain and (right) specific stress–strain compression diagrams

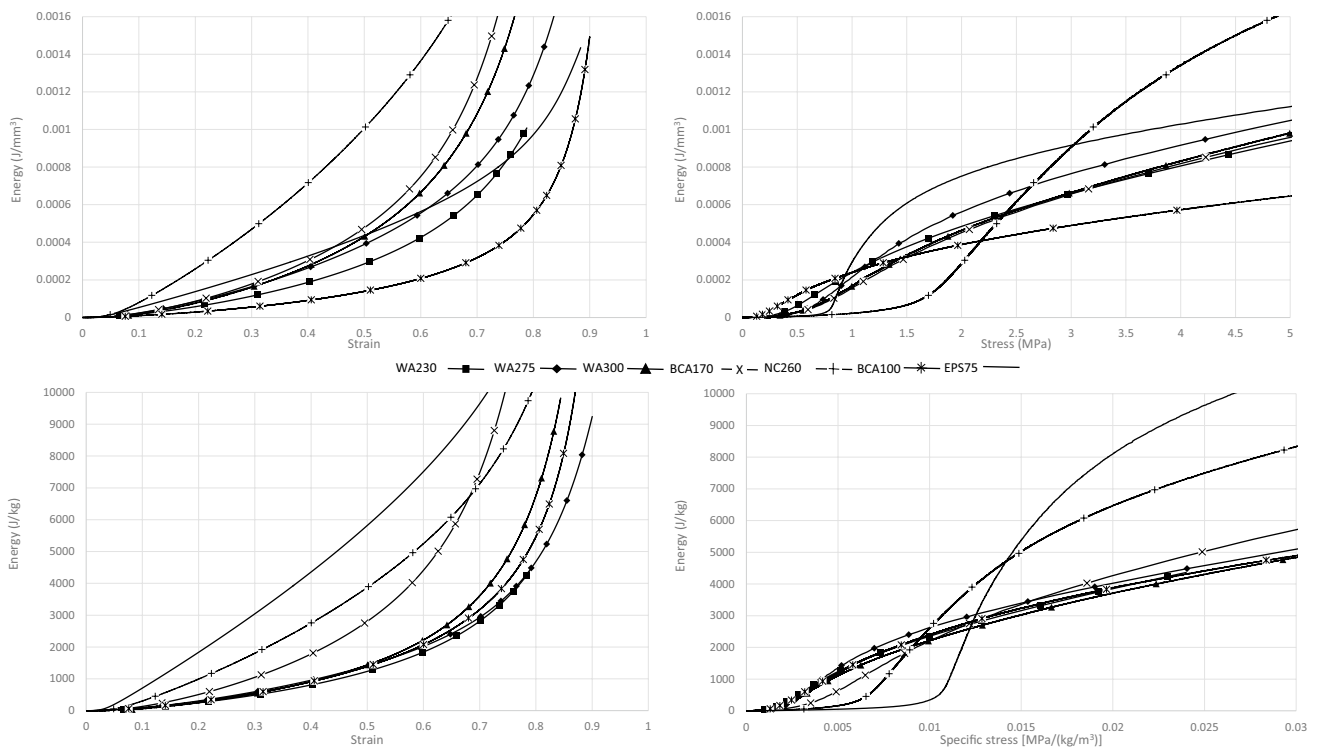
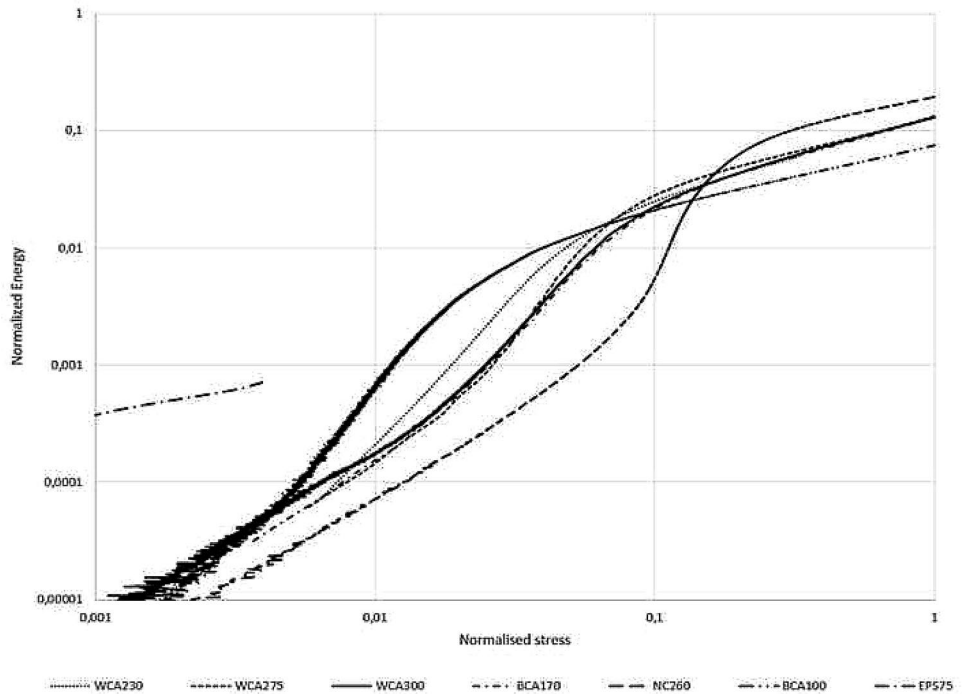


Fig. 7 Energy diagrams: (top-left) energy–strain, (top-right) energy–stress, (bottom-left) specific energy–strain, and (bottom-right) specific energy–stress

Fig. 8 Normalized energy–normalized stress (both axes on a logarithmic scale)



and cork agglomerates than in the EPS as some authors have previously pointed out (Fernandes et al. 2015). A comparison of the different types of WAC shows that, as

some authors have previously noted (Anjos et al. 2014), lower density implies lower stresses in the plateau, a lower Young’s modulus in the elastic zone, and a lower Young’s

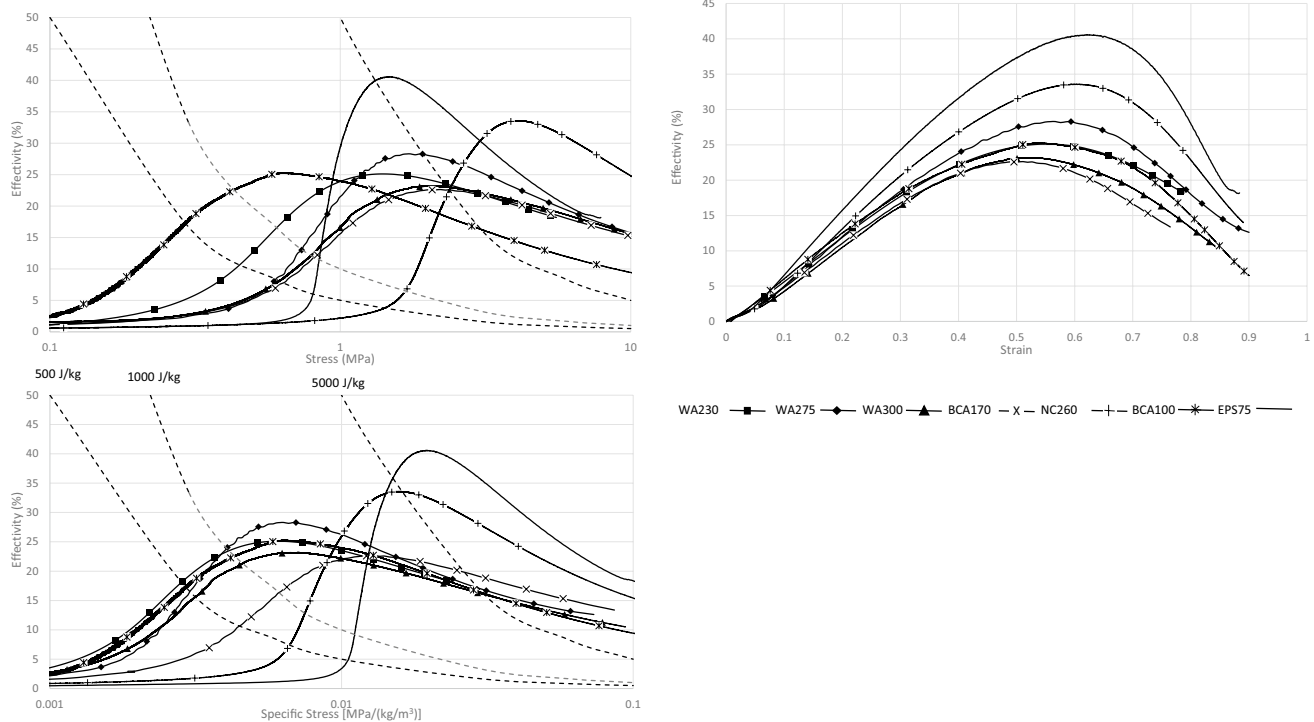


Fig. 9 Efficiency diagrams: (top-left) efficiency-stress (logarithmic scale with iso-energy curves), (top-right) efficiency-strain, and (bottom-left) efficiency-specific stress (logarithmic scale with iso-energy curves)

modulus in the plateau. Additionally, a lower density implies more air trapped inside the material, which causes the densification to appear later.

Although the brown cork agglomerate (BCA170) has a lower density than WCA 300, it exhibits higher mechanical properties. The black agglomerate exhibits the lowest mechanical properties, but densification appears later.

The analysis of the specific mechanical properties (right side of Fig. 6) shows that, except for the BCA170, all the other agglomerates exhibit similar specific mechanical properties, and for those with lower density the densification appears later.

Due to the low density of the EPS, although it does not exhibit the highest mechanical properties, it exhibits the highest specific properties. The natural cork exhibits high specific properties, but due to its high density, these properties are lower than those of the EPS. The natural cork exhibits better specific and nonspecific properties than the agglomerates, which are generated by chopping and blending natural cork. Finally, the BCA170 exhibits high specific mechanical properties. This could be due to the combination of a low density and high grain sizes (see Table 1). There is no remarkable difference in the behaviour of the materials under compressive loads due to the binder. This relationship appears mainly under traction loads (Anjos et al. 2011) and under shear efforts because the binder must join the grains.

Whilst in these diagrams it is also possible to see the absorbed energy which is the area below the stress–strain curve, it can be observed properly in Fig. 7.

The upper-left diagram of Fig. 7 shows that the natural cork can absorb the most energy per unit volume, followed sequentially by BAC170 and WAC300. Moreover, except for the BAC, higher densities imply a higher capability to absorb energy per unit of volume.

An analysis of the bottom-left diagram of Fig. 7 shows that, except for the BAC170, all the agglomerates exhibit a similar capability to absorb energy per unit mass until a certain point where densification appears. Heavier materials generally exhibit earlier densification, so the energy per unit mass increases earlier. These diagrams are useful to select the optimum material to absorb a certain amount of energy per unit volume or per unit mass. The optimum material will be the one that exhibits higher strain without reaching the densification point. The main problem is that it is difficult to establish the densification zone in these diagrams.

The diagrams on the right side of Fig. 7 show the energy per unit volume (top) or per unit mass (bottom) vs the stress on a logarithmic scale. For EPS, Avalle et al. (2001) demonstrated that the same type of polymeric foam has a linearly increasing envelope curve; this curve shows the amount of energy that foam can efficiently absorb. For the agglomerates, it is possible to observe the optimum point, which is

the tangent to the curve that begins in the origin; however, there is not a common envelope. These diagrams can be used to obtain the material that absorbs a certain amount of energy with lower stress, which implies, for instance in the particular case of a helmet, lower forces, and lower decelerations in the brain.

Figure 8 shows the normalized absorbed energy vs. the normalized stress, which is usually used to compare materials, especially foams, obtained from different initial materials, and uses the elastic Young's modulus of the base material (non-expanded polystyrene for EPS and NC for cork agglomerates) for normalization. These diagrams show the peaks and variation between the elastic zone and the plateau zone. The materials with softer curves exhibit softer transitions between both zones. Consequently, the stiffness of the material across the elastic and plateau zones changes less. This behaviour implies lower peak forces and decelerations (Maskery et al. 2017).

In this diagram, some materials have nearly identical curves (WCA 275, WCA 300, and BCA 170), which are similar to the curve for WCA230. These materials exhibit softer curves, which are related to the stress–strain curve in Fig. 6. It can be observed that these are the materials with a softer transition between the elastic and plateau zones. Those materials with sharper transitions, such as NC or BCA, exhibit sharper curves. This is indicative of possible acceleration peaks that should be avoided.

It must be noted that, whilst the diagrams on the right side of Fig. 7 show the most efficient point for each material, this point is difficult to obtain using this diagram and the efficiency diagrams (Fig. 9) are more suitable for this purpose.

These diagrams are useful to determine the most efficient material to absorb a certain amount of energy per unit volume or per unit mass using iso-energy curves that can be easily traced. In the same way, if the maximum stress that we want to reach is known, the most efficient foam can be obtained. For polymeric foams, Avalle et al. (2001) demonstrated with an efficiency–stress diagram that foams with the same cell wall material have equal efficiency, which could be represented with a horizontal envelope curve. For cork, this phenomenon does not occur. It must be highlighted that EPS is the most efficient material followed by natural cork. The other materials exhibit lower efficiency than the EPS; additionally, they exhibit similar efficiency among them (between 28 and 23%). If WCAs are analysed, there is not a clear relationship between the efficiency and the density.

The diagram at the bottom of Fig. 9 shows that, except for the BAC170, all the other agglomerates have the highest efficiency with similar specific stress.

Finally, the efficiency–strain diagram (Fig. 9 right) is plotted to demonstrate that those materials that have later densification points exhibit higher efficiencies, and these efficiencies occur close to these points. Hence, the

efficiency–strain diagram could be used to determine the transition point between the plateau and the densification zone, which is difficult to obtain from the stress–strain curve because the transition is quite diffuse (Gibson and Ashby 1997).

4 Conclusion

The main conclusions obtained from this study are as follows:

- The energy and efficiency diagrams are a suitable tool to select between different types of corks and cork agglomerates based on the required energy absorption or the maximum stress that should not be exceeded.
- The use of specific stress and specific energy allows the selection of materials while considering the weight instead of the volume.
- The main types of cork agglomerates exhibit similar specific stress–strain curves and specific energy absorbed energy–strain curves in the elastic and plateau zones. Additionally, the densification zone appears earlier in heavier agglomerates due to the fact that they have less air trapped inside the grains.
- The main types of cork agglomerates exhibit similar normalized energy–normalized stress curves.
- Natural cork exhibits notably higher nonspecific and specific properties, and cork agglomerate has remarkable properties. However, in natural cork, densification appears earlier.
- The plateau zone for EPS is flat, whereas the natural cork and the cork agglomerates exhibit a constantly increasing curve in this zone. The slope in this curve (Young's modulus in the plateau zone) is directly related to the mechanical properties and the density.
- EPS75, which is a medium-density foam used in helmets, exhibits better nonspecific and, especially, specific properties than the cork agglomerates due to its low density. Additionally, the densification appears later, so the plateau is wider and it can absorb more energy before reaching the densification point.
- The efficiency–strain and efficiency–stress diagrams are useful tools for determining the densification point, which would be reached near the most efficient point.
- In terms of efficiency, EPS exhibits the highest efficiency followed by the natural cork. The agglomerates exhibit similar efficiency, but there is not a clear relationship between the efficiency and the grain size or the density.

- The efficiency is directly related to the densification, so those materials that exhibit later densification also exhibit high efficiency.

In summary, while cork agglomerates are a renewable material, especially due to their high density, their properties are lower than those of EPS. However, this does not mean that they cannot be used in helmets. Nevertheless, these materials will be heavier than EPS, which can negatively affect rotational moments and rotational accelerations. This is an aspect that should be studied in-depth in the future using full-scale models.

Finally, it must be highlighted that the temperature and the impact velocity/strain rate modifies the stress–strain curve and, consequently all the studied parameters. Consequently, a future research line could be the study of the influence of these parameters on the efficiency, ideality, and absorption of energy.

Acknowledgements The author(s) disclose receipt of financial support for the research, authorship, and/or publication of this article: This work was supported by the “Ibercaja Foundation” Young Research Grant. IberDoD HBCU/MI Basic Research Grant (Grant no. JIUZ-2018-TEC-09), the University of Zaragoza (Spain) and the research group ID-ERGO.

Compliance with ethical standards

Conflict of interest This article does not present any conflict of interest.

References

- Anjos O, Pereira H, Rosa ME (2011) Tensile properties of cork in axial stress and influence of porosity, density, quality and radial position in the plank. *Eur J Wood Prod* 69(1):85–91. <https://doi.org/10.1007/s00107-009-0407-0>
- Anjos O, Rodrigues C, Morais J et al (2014) Effect of density on the compression behaviour of cork. *Mater Des* 53:1089–1096. <https://doi.org/10.1016/j.matdes.2013.07.038>
- Avalle M, Belingardi G, Montanini R (2001) Characterization of polymeric structural foams under compressive impact loading by means of energy-absorption diagram. *Int J Impact Eng* 25(5):455–472. [https://doi.org/10.1016/S0734-743X\(00\)00060-9](https://doi.org/10.1016/S0734-743X(00)00060-9)
- Chen W, Hao H, Hughes D et al (2015) Static and dynamic mechanical properties of expanded polystyrene. *Mater Des* 69:170–180. <https://doi.org/10.1016/j.matdes.2014.12.024>
- Chua YS, Law E, Pang SD et al (2017) Impact behaviour and design optimization of a ductile scale-cellular composite structure for protection against localized impact. *Int J Solids Struct* 122:162–174. <https://doi.org/10.1016/j.ijsolstr.2017.06.012>
- Coelho RM, Alves de Sousa RJ, Fernandes FAO et al (2012) New composite liners for energy absorption purposes. *Mater Des* 43:384–392. <https://doi.org/10.1016/j.matdes.2012.07.020>
- Crouvisier-Urien K, Bellat JP, Gougeon RD et al (2018) Mechanical properties of agglomerated cork stoppers for sparkling wines: Influence of adhesive and cork particle size. *Compos Struct* 203:789–796. <https://doi.org/10.1016/j.compstruct.2018.06.116>
- de Sousa RA, Gonçalves D, Coelho R et al (2012) Assessing the effectiveness of a natural cellular material used as safety padding material in motorcycle helmets. *Simul Trans Soc Model Simul Int* 88(5):580–591. <https://doi.org/10.1177/0037549711414735>
- Delucia M, Catapano A, Montemurro M, Pailhès J (2020a) A stochastic approach for predicting the temperature-dependent elastic properties of cork-based composites. *Mech Mater* 145:103399. <https://doi.org/10.1016/j.mechmat.2020.103399>
- Delucia M, Catapano A, Montemurro M, Pailhès J (2020b) Determination of the effective thermoelastic properties of cork-based agglomerates. *J Reinf Plast Compos* 38(16):760–776. <https://doi.org/10.1177/0731684419846991>
- Doroudiani S, Kortschot MT (2003) Polystyrene foams. III. Structure–tensile properties relationships. *J Appl Polym Sci* 90(5):1427–1434. <https://doi.org/10.1002/app.128306>
- Fernandes FAO, Jardim RT, Pereira AB et al (2015) Comparing the mechanical performance of synthetic and natural cellular materials. *Mater Des* 82:335–341. <https://doi.org/10.1016/j.matdes.2015.06.004>
- Fernandes FAO, Alves de Sousa RJ, Ptak M et al (2019) Helmet design based on the optimization of biocomposite energy-absorbing liners under multi-impact loading. *Appl Sci-Basel* 9(4):735. <https://doi.org/10.3390/app9040735>
- Gibson LJ, Ashby MF (1997) Cellular solids: structures and properties. Cambridge University Press, Cambridge. <https://doi.org/10.1017/CBO9781139878326>
- González-Hernández F, González-Adrados JR, García de Ceca L et al (2014) Quality grading of cork stoppers based on porosity, density and elasticity. *Eur J Wood Prod* 72(2):149–156. <https://doi.org/10.1007/s00107-013-0760-x>
- Hajiaghameh M, Seidi M, Margulies SS (2020) Head rotational kinematics, tissue deformations, and their relationships to the acute traumatic axonal injury. *J Biomech Eng* 142(3):031006. <https://doi.org/10.1115/1.4046393>
- Hanssen AG, Langseth M, Hopperstad OS (1999) Static crushing of square aluminium extrusions with aluminium foam. *Int J Mech Sci* 24(4):147–383. [https://doi.org/10.1016/S0020-7403\(98\)00064-2](https://doi.org/10.1016/S0020-7403(98)00064-2)
- Hanssen AG, Langseth M, Hopperstad OS (2000) Static and dynamic crushing of square aluminium extrusions with aluminium foam. *Int J Impact Eng* 24(3):347–383. [https://doi.org/10.1016/S0734-743X\(99\)00169-4](https://doi.org/10.1016/S0734-743X(99)00169-4)
- Jardim RT, Fernandes FAO, Pereira AB, Alves de Sousa RJ (2015) Static and dynamic mechanical response of different cork agglomerates. *Mater Des* 68:121–126. <https://doi.org/10.1016/j.matdes.2014.12.016>
- Knapic S, Oliveira V, Machado JS et al (2016) Cork as a building material: a review. *Eur J Wood Prod* 74(6):775–791. <https://doi.org/10.1007/s00107-016-1076-4>
- Lagorce-Tachon A, Karbowski T, Champion D et al (2017) Mechanical properties of cork: effect of hydration. In: Conference: 6th biot conference on poromechanics, Paris, France. <https://doi.org/10.1016/j.matdes.2015.05.034>
- Lauw A, Oliveira V, Lopes F et al (2018) Variation of cork quality for wine stoppers across the production regions in Portugal. *Eur J Wood Prod* 76(1):123–132. <https://doi.org/10.1007/s00107-017-1196-5>
- Le Barbenchon L, Girardot J, Kopp JB, Viot P (2019) Multi-scale foam: 3D structure/compressive behaviour relationship of agglomerated cork. *Materialia* 5:100219. <https://doi.org/10.1016/j.mtla.2019.100219>
- Maderuelo-Sanz R, Barrigón-Morillas JM, Gómez-Escobar V (2014) The performance of resilient layers made from cork granulates mixed with resins for impact noise reduction. *Eur J Wood Prod* 72(6):833–835. <https://doi.org/10.1007/s00107-014-0845-1>
- Maskery I, Aboulkhair NT, Aremu AO et al (2017) Compressive failure modes and energy absorption in additively manufactured double

- gyroid lattices. *Addit Manuf* 16:24–29. <https://doi.org/10.1016/j.addma.2017.04.003>
- Miltz J, Ramon O (1990) Energy absorption characteristics of polymeric foams used as cushioning materials. *Polym Eng Sci* 30(2):129–133. <https://doi.org/10.1002/pen.760300210>
- Oliveira V, Emilia-Rosa M, Pereira H (2014) Variability of the compression properties of cork. *Wood Sci Technol* 48(5):937–948. <https://doi.org/10.1007/s00226-014-0651-2>
- Paiva D, Magalhaes FD (2018) Dynamic mechanical analysis and creep-recovery behavior of agglomerated cork. *Eur J Wood Prod* 76(1):134–141. <https://doi.org/10.1007/s00107-017-1158-y>
- Ptak M, Kaczynski P, Alvesde FFAO, Sousa RJ (2017) Assessing impact velocity and temperature effects on crashworthiness properties of cork material. *Int J Impact Eng* 106:238–248. <https://doi.org/10.1016/j.ijimpeng.2017.04.014>
- Ptak M, Kaczyński P, Wilhelm J, Fernandes F et al (2018) High-energy impact testing of agglomerated cork at extremely low and high temperatures. *Int J Impact Eng* 126:109–116. <https://doi.org/10.1016/j.ijimpeng.2018.12.001>
- Rush KC (1969) Load compression behavior of flexible foams. *J Appl Polym Sci* 52(4):549–568. <https://doi.org/10.1002/app.1969.070131106>
- Rush KC (1970a) Energy-absorbing characteristics of foamed polymers. *J Appl Polym Sci* 16(1):108–122. <https://doi.org/10.1002/app.1970.070140603>
- Rush KC (1970b) Load compression behavior of brittle foams. *J Appl Polym Sci* 14(5):1263–2000. <https://doi.org/10.1002/app.1970.070140514>
- Sanchez-Saez S, García-Castillo SK, Barbero E, Cirne J (2015) Dynamic crushing behaviour of agglomerated cork. *Mater Des* 65:743–748. <https://doi.org/10.1016/j.matdes.2014.09.054>
- Santos PT, Pinto S, Marques PAAP et al (2017) Agglomerated cork: a way to tailor its mechanical properties. *Compos Struct* 178:277–287. <https://doi.org/10.1016/j.compstruct.2017.07.035>
- Silva SP, Sabino MA, Fernandes EM et al (2005) Cork: properties, capabilities and applications. *Int Mater Rev* 53(4):256–256. <https://doi.org/10.1179/174328008X353529>
- Tay YY, Lim CS, Lankarani HM (2014) A finite element analysis of high-energy absorption cellular materials in enhancing passive safety of road vehicles in side-impact accidents. *Int J Crashworthiness* 20(2):210–210. <https://doi.org/10.1080/13588265.2014.893789>
- Wilhelm J, Ptak M, Rusiński E (2017) Simulated depiction of head and brain injuries in the context of cellularbased materials in passive safety devices. *Sci J Maritime Univ Szczecin* 50(122):98–104. <https://doi.org/10.17402/222>
- Yu S, Sun J, Bai J (2019) Investigation of functionally graded TPMS structures fabricated by additive manufacturing. *Mater Des*. <https://doi.org/10.1016/j.matdes.2019.108021>

Publisher's Note Springer Nature remains neutral with regard to jurisdictional claims in published maps and institutional affiliations.